journal

J. Am. Ceram. Soc., 94 [5] 1477–1482 (2011)
DOI: 10.1111/j.1551-2916.2010.04261.x

Preparation and Luminescence Property of Red-Emitting Hardystonite Phosphors by Near-Ultraviolet Irradiation

Shanshan Yao, Lihong Xue,† Youwei Yan, and Mifang Yan

State Key Laboratory of Materials Processing and Die & Mould Technology, College of Materials Science and Engineering, Huazhong University of Science & Technology, Wuhan 430074, China

$A_{1.95}ZnSi_2O_7:Eu^{3+}_{0.05}$ (A = Ca, Sr, Ba) red phosphors were prepared by combustion-assisted synthesis method and their efficient red emission under near ultraviolet (UV) were observed. The luminescence and crystallinity were investigated using luminescence spectrometry and X-ray diffractometer, respectively. The emission spectrum shows that the most intense peak is located at 614 nm, which corresponds to the $^5D_0 \rightarrow {}^7F_2$ transition of Eu^{3+}. These phosphors have two main excitation peaks located at 394 and 465 nm, which match the emission of UV and blue light-emitting diodes, respectively. Thus, these phosphors could be used as red components for white light-emitting diodes.

I. Introduction

The white light-emitting diodes (WLEDs) have attracted considerable attention for use an illuminator for solid-state lighting. WLEDs show high potential for replacement of conventional incandescent and fluorescent lamps, the advantages being it's longtime, saving energy, reliability, and safety.[1]

Up to now, three-band WLEDs were proposed to achieve the combination of the blue GaN-based LED with green and red phosphors, or the pumping of tri-color (red, green, and blue) phosphors with ultraviolet (UV) or violet LED.[2–7] Three-band WLEDs maintain a very high color-rendering index and were believed to offer the greatest potential for high-efficiency solid-state lighting.[8] For excellent color-rendering index, both methods need efficient red phosphors that should have the excitation wavelength matching with the emission wavelength of the blue LEDs (λ_{em} = 440–470 nm) or the near UV-LEDs (λ_{em} = 350–420 nm). The presently used red phosphors for blue and GaN-based LED are commercially still limited to divalent Eu ion activated alkaline earth binary sulfides and $Y_2O_3S:Eu^{3+}$, respectively. However, these sulfides-based phosphors are chemically unstable and the lifetimes of these materials are inadequate, and their luminescent intensities are very low relative to blue and green phosphors. The luminescence intensities of these materials are very low relative to blue and green phosphor. Hence, the search for stable red phosphors with intense excitation in the near-UV/blue spectra region is an urgent need to increase the overall white light efficiency and lifetime.[9]

The trivalent europium ion as a red luminescent activator in many host materials has been studied intensively.[10–15] Major emissions are centered at 590 nm ($^5D_0 \rightarrow {}^7F_1$) and 616 nm ($^5D_0 \rightarrow {}^7F_2$), corresponding well to orange and red color, respectively. So, the relative intensities of $^5D_0 \rightarrow {}^7F_2$ to $^5D_0 \rightarrow {}^7F_1$ transitions in phosphors are important for their applications.[16] In order to obtain red phosphors with high color purity, it is necessary to increase the relative intensity of $^5D_0 \rightarrow {}^7F_2$ to $^5D_0 \rightarrow {}^7F_1$ transitions. It is well known that the relative intensities of the $^5D_0 \rightarrow {}^7F_2$ to $^5D_0 \rightarrow {}^7F_1$ transitions strongly depend on the local symmetry of Eu^{3+} ions.[17–19] The peak at 616 nm is due to the forced electric dipole transition ($^5D_0 \rightarrow {}^7F_2$), in which transition is associated with a relatively low local symmetry of Eu^{3+} ions. The better color purity might result from the more distorted lattices and relatively lower crystal symmetry. Consequently, a change of the crystal structure of host materials can produce a good red phosphor.[20]

Recently, silicates phosphors have become important luminescent materials because of its excellent thermal and charge stabilization. The hardystonites are represented as $A_2ZnSi_2O_7$, where A is an alkaline earth. There are only a few studies related to their optical properties. Herein, we synthesized the $A_2ZnSi_2O_7:Eu^{3+}$ (A = Ca, Sr, Ba) red-emitting phosphors by the combustion-assisted synthesis method and investigated their luminescent properties.

II. Experimental Procedure

$A(NO_3)_2$ (A = Ca, Sr, Ba)(AR), $Zn(NO_3)_2 \cdot 6H_2O$(AR), $Si(OC_2H_5)_4$(AR), Eu_2O_3 (99.99%) were employed as the raw materials (all these materials being analytical grade). NH_2CONH_2(AR) was added as a fuel and small quantities of H_3BO_3(AR) as a flux, respectively. Eu_2O_3 was dissolved in HNO_3 to convert into $Eu(NO_3)_3$ solution completely. The raw materials were weighed as the optimal nominal composition as reported previously.[21] Then a suitable volume of deionized matter and stoichiometric amount of $A(NO_3)_2$, $Zn(NO_3)_2 \cdot 6H_2O$, NH_2CONH_2 and small quantities of H_3BO_3 were added to form a clear solution. A stoichiometric amount of $Si(OC_2H_5)_4$ dissolved in ethanol was added dropwise into the above solution under vigorous stirring. $Si(OH)_4$ was formed by the hydrolysis of $Si(OC_2H_5)_4$ as follows:

$$n\mathrm{Si(OC_2H_5)_4} + 4n\mathrm{H_2O} \rightarrow n\mathrm{Si(OH)_4} + 4n\mathrm{C_2H_5OH}$$

The mixture solution was allowed to react at 80°C for 2 h to obtain a homogenous solution. And then the solution was introduced into a muffle furnace preheated at 600°C. Within a few minutes, the solution boiled and was ignited to produce a self-propagating flame. The product obtained was postannealed at 1000°C for 3 h.

The synthesized phosphors were ground to a powder and passed through a 200-mesh sieve before the characterization. The crystal phase of the synthesized powders prepared was characterized by X-ray powder diffraction using an X′Pert PRO (Almelo, the Netherlands) X-ray diffractometer having a Cu$K\alpha$ radiation (λ = 1.5406 Å) at 40 kV tube voltage and 40 mA tube current. The XRD patterns were collected in the range of $10° \leq 2\theta \leq 90°$. The emission spectrum was measured on a RF-5301 fluorescence spectrophotometer (Shimadzu, Tokyo, Japan) equipped with a xenon discharge lamp as an excitation source.

J. Ballato—contributing editor

Manuscript No. 28257. Received June 29, 2010; approved October 19, 2010.

This work was financially supported by the Natural Science Foundation of China (No.51002054), the Natural Science Foundation of Hubei Province of China (No.2008CB252), the Fundamental Research Funds for the Central Universities (C2009Q012) and by the Scientific Research Foundation for the Returned Overseas Chinese Scholar, State Education Ministry.

†Author to whom correspondence should be addressed. e-mail: xuelh@mail.hust.edu.cn

The excitation and emission slits were set to 3.0 nm. All the above measurements were taken at room temperature.

The chromaticity coordinates were obtained according to the Commission International de l′Eclairage (CIE) using a Spectra Lux Software v.2.0 Beta.[22]

III. Results and discussion

The tetragonal crystal structure of $A_2BSi_2O_7$ was first reported by Kimata, where A = Ca and B = Co.[23] The compositions $Sr_2MgSi_2O_7$, $Ca_2ZnSi_2O_7$, $Sr_2ZnSi_2O_7$, etc., belonging to the $A_2BSi_2O_7$ series have a tetragonal crystal structure.[24,25] Some of the other silicates in $A_2BSi_2O_7$ series like $Ba_2ZnSi_2O_7$, $Ba_2MgSi_2O_7$, and $Ba_2CuSi_2O_7$ crystallize in the monoclinic structure.[26–28] The crystal structure of the tetragonal form of $A_2ZnSi_2O_7$ (A = Ca, Sr) is shown in Figs. 1(a) and (b). It contains discrete $[Si_2O_7]^{6-}$ units formed by two corner-sharing SiO_4 tetrahedrals. The Zn atoms lie in the tetrahedral formed by oxygen atoms while the A^{2+} (A = Ca, Sr) cations have an eightfold oxygen coordination. The crystal structure of the monoclinic form of $Ba_2ZnSi_2O_7$ is shown in Fig. 1(c). It consists of $[ZnO_4]$ tetrahedral, which share their oxygen atoms with those of the $[Si_2O_7]$ groups, thus forming two-dimensionally infinite sheets that are separated by the Ba atoms.

Figure 2 shows the XRD patterns of $A_{1.95}ZnSi_2O_7:Eu^{3+}_{0.05}$ (A = Ca, Sr, Ba) ceramic phosphors. Figures 2(a) and (b) patterns obtained can be indexed according to the JCPDS files card no.: 75-0916 and 39-0235 for $Ca_2ZnSi_2O_7$ and $Sr_2ZnSi_2O_7$ having hardystonite-type structure (tetragonal) with the space group $P\bar{4}2_{1m}$ (no. 113). Figure 2(c) shows the XRD patterns for $Ba_{1.95}ZnSi_2O_7:Eu^{3+}_{0.05}$, which is indexed according to JCPDS file card no.: 86-0769 for $Ba_2CoSi_2O_7$ having a monoclinic structure with the space group $C2/c$ (no. 15).[26] The lattice parameters listed inTable I shows that there is good agreement between the literature and the prepared $A_2ZnSi_2O_7$ and $A_{1.95}ZnSi_2O_7:Eu^{3+}_{0.05}$ (A = Ca, Sr, Ba) samples values, suggesting that the method starting from the silicates is successfully applied here. Meanwhile, it is clear that the Eu^{2+} doping ions do not change the general structure.

An acceptable percentage difference in ion radii between doped and substituted ions must not exceed 30%.[29] The calculations of the radius percentage difference (D_r) between the doped Eu^{3+} ions and the possible substituted ions (A^{2+} [A = Ca, Sr, Ba], Zn^{2+}) in $A_2ZnSi_2O_7$ (A = Ca, Sr, Ba) are summarized in Table II. The values are based on the following formula[30]:

$$D_r = \frac{[R_m(CN) - R_d(CN)]}{R_m(CN)} \quad (1)$$

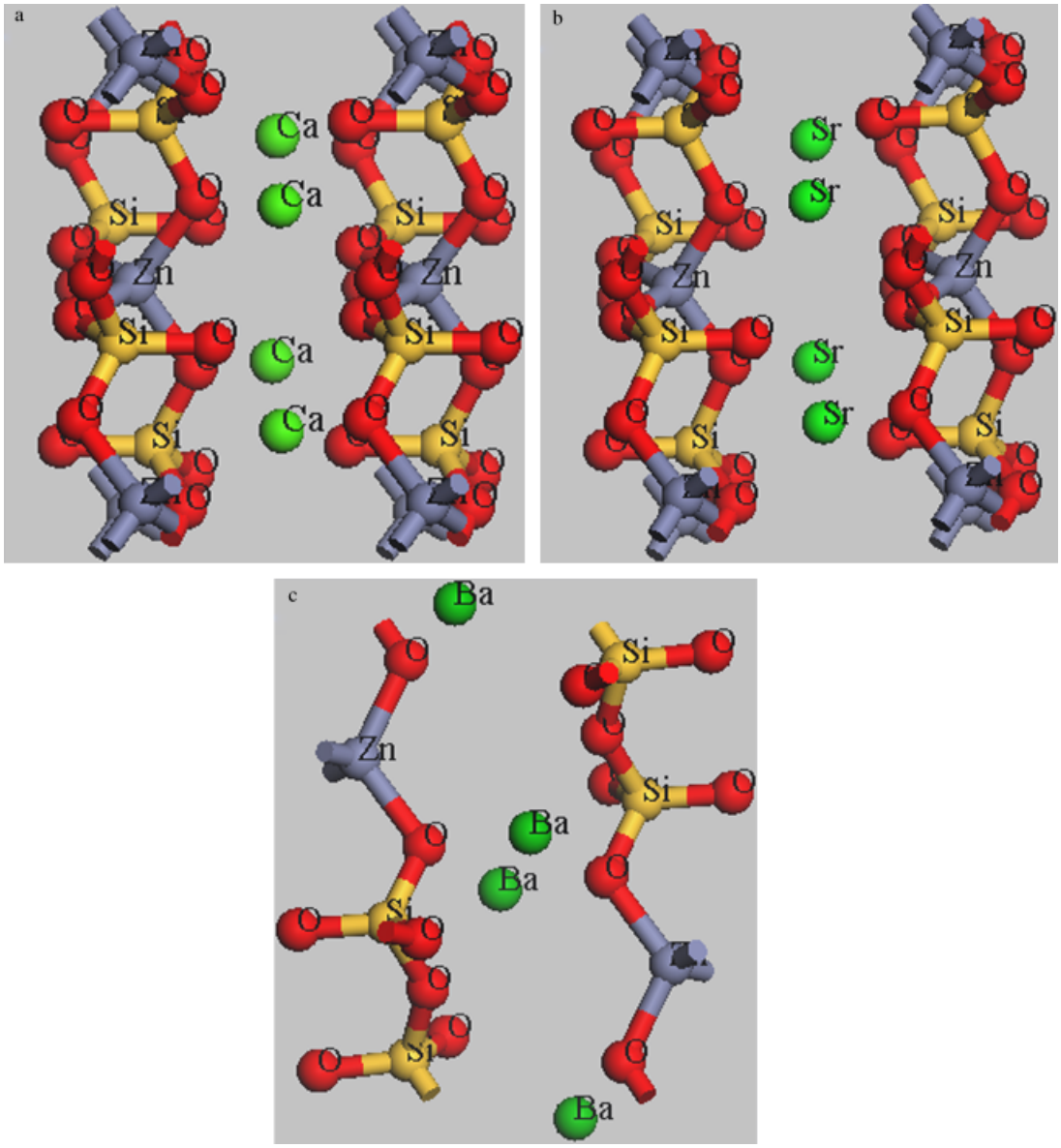

Fig. 1. The crystal structure of (a, b) the tetragonal form of $A_2ZnSi_2O_7$ (A = Ca, Sr) and (c) the monoclinic form of $Ba_2ZnSi_2O_7$.

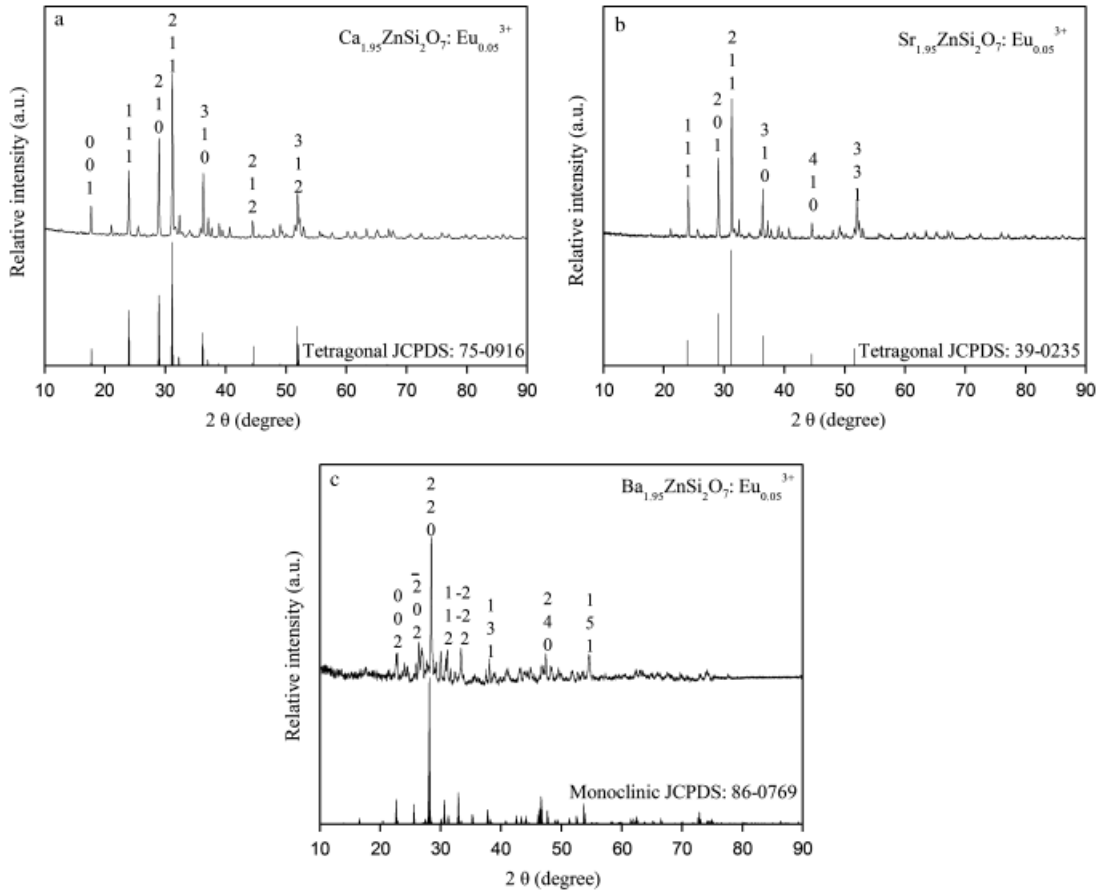

Fig. 2. X-ray diffraction patterns of (a) $Ca_{1.95}ZnSi_2O_7:Eu^{3+}_{0.05}$, (b) $Sr_{1.95}ZnSi_2O_7:Eu^{3+}_{0.05}$ and (c) $Ba_{1.95}ZnSi_2O_7:Eu^{3+}_{0.05}$ ceramic phosphors.

where CN is the coordination number, R_m(CN) is the radius of host cation, and R_d(CN) is the radius of doped ion. We take the data of Eu^{3+} with CN = 6 as a responsible approximation.[32] The values of D_r between Eu^{3+} occupied alkaline earth metal ions (A = Ca, Sr, Ba) sites are 4.46%, 15.08% and 24.65%, respectively, while D_r between Eu^{3+} and Zn^{2+} (or Si^{4+}) is −58.33% (or −265.38%). Obviously, the doping ions of Eu^{3+} will clearly substitute the alkaline earth metal ions (A = Ca, Sr, Ba) sites.

As trivalent Eu^{3+} ions are doped into $A_2ZnSi_2O_7$ (A = Ca, Sr, Ba), they would nonequivalently replace the alkaline earths ions. In order to keep the charge balance, two Eu^{3+} ions would be needed to substitute for three alkaline earths ions (the total charge of two trivalent Eu^{3+} ions is equal to that of three alkaline earths ions). Hence, one vacancy defect of V''_A (A = Ca, Sr, Ba) with two negative charges, and two positive defects of $Eu^{\bullet}_A$ (A = Ca, Sr, BA) would be created by each substitution of every two Eu^{3+} ions in the compound. The vacancy V''_A would act as a donor of electrons, while the two $Eu^{\bullet}_A$ defects become acceptors of the electrons. Consequently, the negative charges in the vacancy defects of V''_A would be transferred to the Eu^{3+} sites. The whole process can be expressed by the following equation[33]:

$$3A^{2+}(A = Ca, Sr, Ba) + 2Eu^{3+} \rightarrow V''_A + 2Eu^{\bullet}_A$$

$$V''_A \rightarrow V^x_A + 2e$$

$$2Eu^{\bullet}_A + 2e \rightarrow 2Eu^x_A$$

The excitation spectra of $A_{1.95}ZnSi_2O_7:Eu^{3+}_{0.05}$ are measured in the wavelength range of 300–500 nm by monitoring with the intense red emission located at 614 nm (Fig. 3). The excitation spectra consist of two intense bands at 394 and 465 nm in addition to four relatively weak bands peaking about 320, 362, 383, and 416 nm. The bands peaking around 320, 362, 394 and 465 nm are assigned to transition from the $^7F_0$ level to the $^3H_4$, $^5D_4$, $^5L_6$, and $^5D_2$ levels of *f–f* transitions of Eu^{3+}, respectively. On the other hand, rest of the bands peaking around 383 and 416 nm are assigned to the transitions from the thermal populated $^7F_1$ level to the $^5F_4$ and $^5L_6$.[34,35] The strong broad band peaking at 394 nm and the narrow band at 465 nm correspond to the characteristic

Table I. Lattice Parameters Values of $A_2ZnSi_2O_7:Eu^{3+}_{0.05}$ (A = Ca, Sr, Ba) Phosphors Calculated from the XRD Pattern

Samples	*a* (Å)	*b* (Å)	*c* (Å)	*V* (Å^3)
$Ca_{0.95}Zn_2Si_2O_7:Eu^{3+}_{0.05}$	7.649	7.649	5.078	297.10
JCPDS (75-0916)	7.830	7.830	4.990	305.93
$Sr_{0.95}Zn_2Si_2O_7:Eu^{3+}_{0.05}$	7.763	7.763	5.130	309.16
JCPDS (39-0235)	8.002	8.002	5.170	331.10
$Ba_{0.95}Zn_2Si_2O_7:Eu^{3+}_{0.05}$	8.338	10.560	8.338	696.33
JCPDS (86-0769)	8.434	10.722	8.436	710.75

Table II. Ionic Radii Difference Percentage (D_r) Between Matrix Cations and Doped Ions

		$D_r = [R_m(CN)–R_d(CN)]/R_m(CN)$ (%)				
Doped ions	R_d (CN) (Å)	$R^{2+}_{Ca}(8)$ = 1.12 (Å)	$R^{2+}_{Sr}(8)$ = 1.26 (Å)	$R^{2+}_{Ba}(8)$ = 1.42 (Å)	$R^{2+}_{Zn}(4)$ = 0.60 (Å)	$R^{4+}_{Si}(4)$ = 0.26 (Å)
Eu^{3+}	0.95 (6) 1.07 (8)	4.46	15.08	24.65	−58.33	−265.38

CN stands for coordination number, R_m (CN) and R_d (CN) for the radii of matrix and doped cations, respectively, and the data of the effective ionic radii are from Liebau.[31]

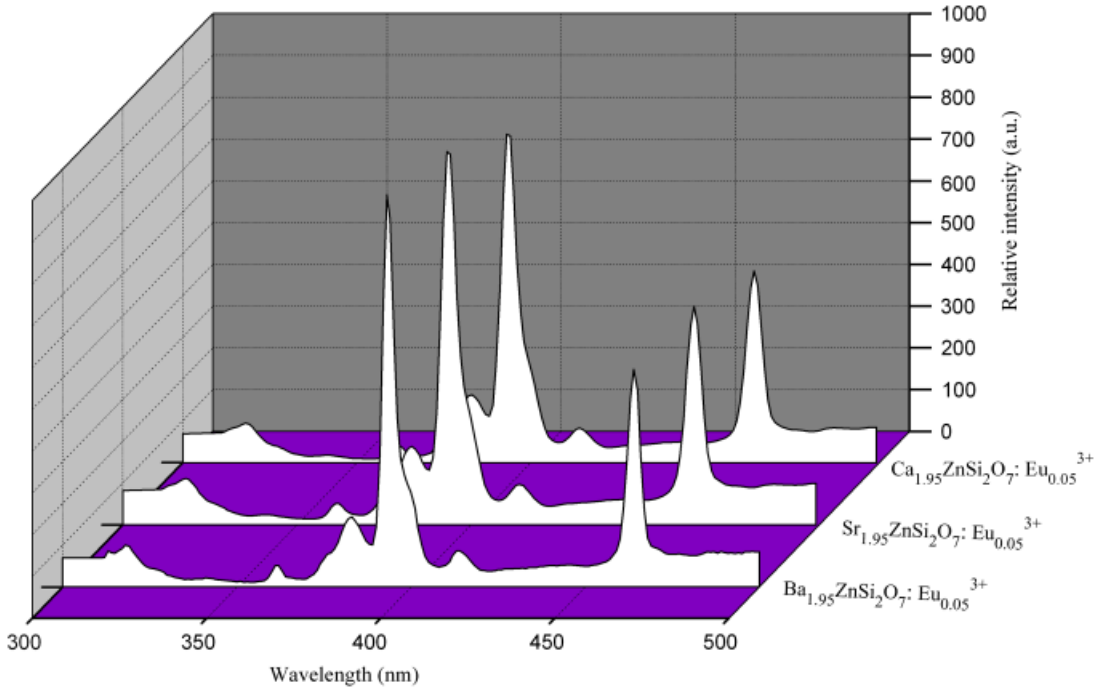

Fig. 3. Excitation intensity ($\lambda_{em} = 614$ nm) of $A_{1.95}ZnSi_2O_7:Eu^{3+}_{0.05}$ (A = Ca, Sr, Ba) phosphors.

f–f transitions of Eu^{3+} within its $^4f_6$ configuration. From above observations, the codopant Eu^{3+} ions are substituted for the alkaline earth metal ions (A = Ca, Sr, Ba) sites.

Figure 4 shows the emission spectral of as-synthesized Eu^{3+}-doped $A_2ZnSi_2O_7$ phosphors. The spectrum exhibits five emission peaks at 579, 591, 614, 652, and 703 nm. These five emission peaks can be attributed to the $^5D_0 \rightarrow {}^7F_{0,1,2,3,4}$ transitions of Eu^{3+}.[36,37] All of them consist of two main peaks centered at 591 and 614 nm, which come from the transitions of $^5D_0 \rightarrow {}^7F_1$ and $^5D_0 \rightarrow {}^7F_2$, respectively. The most intense emission is the $^5D_0 \rightarrow {}^7F_2$ transition located in 614 nm, corresponding to the red emission, in good accordance with the Judd–Ofelt theory.[38] Therefore, strong red emission can be observed. The main excitation peaks indicate that these phosphors are very suitable as a color converter using UV lights as the primary light source. It can be used as red phosphors excited by UV-LED chip and would have applications in the solid-state lighting field.

The main highest emission peak is located at around 614 nm for all samples without a visible shift, caused by $^5D_0 \rightarrow {}^7F_2$, which is a hypersensitive forced electric dipole transition.[39] It is known that the emission wavelengths of Eu^{3+} are determined primarily by their local environment in host crystallites. The intensity ratio of $^5D_0 \rightarrow {}^7F_2$ to $^5D_0 \rightarrow {}^7F_1$, also called the asymmetric ratio, is close to being related to the local environment of Eu^{3+}.[40] Generally, the larger the intensity ratio of $^5D_0 \rightarrow {}^7F_2$ to $^5D_0 \rightarrow {}^7F_1$, the lower the local symmetry.[41] The asymmetric

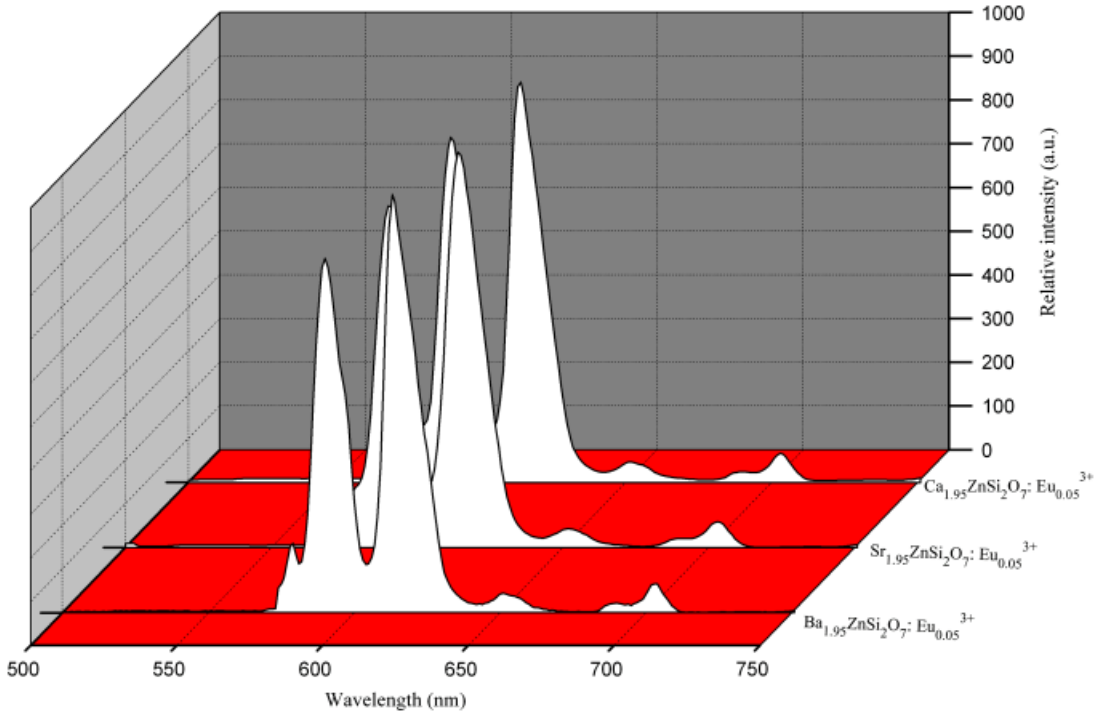

Fig. 4. Emission intensity ($\lambda_{ex} = 394$ nm) of $A_{1.95}ZnSi_2O_7:Eu^{3+}_{0.05}$ (A = Ca, Sr, Ba) phosphors.

Table III. Asymmetric Ratios of I [$^5D_0 \rightarrow {}^7F_2$]/$I$ [$^5D_0 \rightarrow {}^7F_1$] of $A_{1.95}ZnSi_2O_7:Eu^{3+}_{0.05}$ (A = Sr, Ca, Ba)

Samples	*Asymmetric ratio I [$^5D_0 \rightarrow {}^7F_2$]/$I$ [$^5D_0 \rightarrow {}^7F_1$]
$Sr_{1.95}ZnSi_2O_7:Eu^{3+}_{0.05}$	870/808 = 1.08
$Ca_{1.95}ZnSi_2O_7:Eu^{3+}_{0.05}$	906/815 = 1.11
$Ba_{1.95}ZnSi_2O_7:Eu^{3+}_{0.05}$	964/820 = 1.18

*I [$^5D_0 \rightarrow {}^7F_2$] was calculated from photoluminescent intensities at 614 nm, while [$^5D_0 \rightarrow {}^7F_1$] was calculated from intensities at 591 nm.

ratios of $A_{1.95}ZnSi_2O_7:Eu^{3+}_{0.05}$ (A = Sr, Ca, Ba) particles were also calculated, and the results are shown in Table III . The results show that the asymmetric ratio increase slightly, which confirms the decrease in local symmetry. The fluorescence intensity ratio of $^5D_0 \rightarrow {}^7F_2$ to $^5D_0 \rightarrow {}^7F_1$ transitions of Eu^{3+} increases with increasing ionic radius in the order of Sr < Ca < Ba for hardystonite.[42–45] So, in the three hardystonite phosphors, $Ba_{1.95}ZnSi_2O_7:Eu^{3+}_{0.05}$ has the strongest emission intensity.

Color purity can be visualized in the chromaticity diagram (Fig. 5), with the emission color coordinates of the luminescent material. The CIE chromaticity diagram of $A_{1.95}ZnSi_2O_7:Eu^{3+}_{0.05}$ (A = Ca, Sr, Ba) samples were obtained using a Spectra Lux Software v.2.0 Beta.[22] For any given color there is one setting for each three numbers X, Y, and Z known as tristimulus values that will produce a match. Based on emission spectrum of $A_{1.95}ZnSi_2O_7:Eu^{3+}_{0.05}$ (A = Ca, Sr, Ba) samples, the (x, y) color coordinates were determined with the following values (x, y) = (0.489, 0.355), (0.466, 0.353), and (0.576, 0.362), respectively.

IV. Conclusion

The $A_2ZnSi_2O_7:Eu^{3+}$ (A = Ca, Sr, Ba) red phosphors were prepared by the combustion-assisted synthesis method. In the three crystal structures, the doping ions of Eu^{3+} will clearly substitute the alkaline earth metal ions. $Ba_{1.95}ZnSi_2O_7:Eu^{3+}_{0.05}$ has the strongest emission intensity by the lowest local symmetry.

The CIE of the $Ca_{1.95}ZnSi_2O_7:Eu^{3+}_{0.05}$, $Sr_{1.95}ZnSi_2O_7:Eu^{3+}_{0.05}$, and $Ba_{1.95}ZnSi_2O_7:Eu^{3+}_{0.05}$ sanples were calculated (x, y) = (0.489, 0.355), (0.466, 0.353), and (0.576, 0.362). These excitation spectra couple well with the emission of UV-LED (350–410 nm).

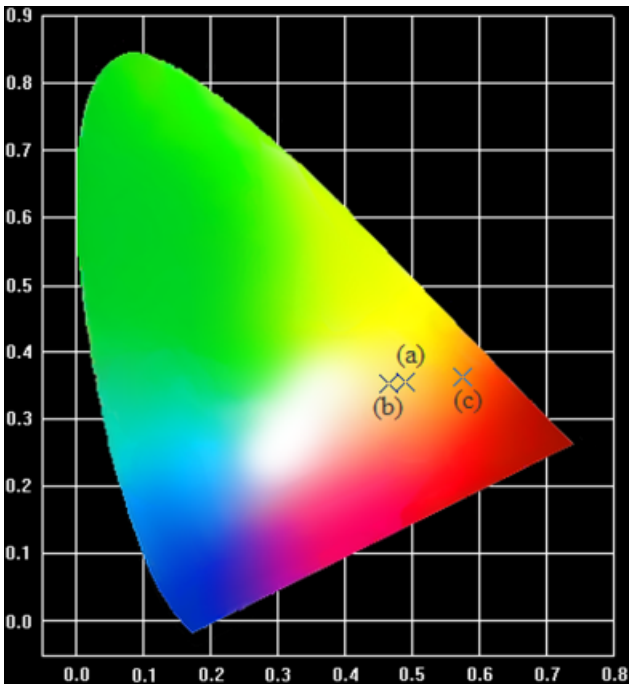

Fig. 5. CIE diagram of (a) $Ca_{1.95}ZnSi_2O_7:Eu^{3+}_{0.05}$, (b) $Sr_{1.95}ZnSi_2O_7:Eu^{3+}_{0.05}$, and (c) $Ba_{1.95}ZnSi_2O_7:Eu^{3+}_{0.05}$ ceramic phosphors (λ_{ex} = 394 nm).

The results indicate that these hardystonite phosphors are very suitable for color converter using UV lights as the primary light source.

References

[1]M. Dyble, N. Narendran, A. Bierman, and T. Klein, "Impact of Dimming White LEDs: Chromaticity Shifts Due to Different Dimming Methods," *Proc. SPIE*, **5941**, 291–9 (2005).

[2]H. A. Höppe, "Recent Developments in the field of Inorganic Phosphors," *Angew. Chem. Int. Ed.*, **48**, 3572–82 (2009).

[3]C. Feldmann, T. Jüstel, C. R. Ronda, and P. J. Schmidt, "Inorganic Luminescent Materials: 100 Years of Research and Application," *Adv. Funct. Mater.*, **13**, 511–6 (2003).

[4]E. Danielson, M. Devenney, D. M. Giaquinta, J. H. Golden, R. C. Haushalter, E. W. McFarland, D. M. Poojary, C. M. Reaves, W. H. Weinberg, and X. D. Wu, "A Rare-Earth Phosphor Containing One-Dimensional Chains Identified Through Combinatorial Methods," *Science*, **279**, 837–9 (1998).

[5]E. Danielson, J. H. Golden, E. . W McFarland, C. M. Reaves, W. H. Weinberg, and X. D. Wu., "A Combinatorial Approach to the Discovery and Optimization of Luminescent Materials," *Nature*, **389**, 944–8 (1997).

[6]J. Liu and Y. D. Li, "Synthesis and Self-Assembly of Luminescent Ln^{3+}-Doped $LaVO_4$ Uniform Nanocrystals," *Adv. Mater.*, **19**, 1118–22 (2007).

[7]C. F. Guo, W. Zhang, L. Luan, T. Chen.H.Cheng, and D. X. Huang, "A Promising Red-Emitting Phosphor for White Light Emitting Diodes Prepared by Sol–Gel Method," *Sensor Actuat. B-Chem.*, **133**, 33–9 (2008).

[8]J. K. Sheu, S. J. Chang, C. H. Kuo, Y. K. Su, K. W. Wu, Y. C. Lin, W. C. Lai, J. M. Tsai, G. C. Chi, and R. K. Wu, "White-Light Emission from Near UV InGaN–GaN LED Chip Precoated with Blue/Green/Red Phosphors," *IEEE Photon. Echnol. Lett.*, **15**, 18–20 (2003).

[9]V. Sivakumar and U. V. Varadaraju, "Intense Red-Emitting Phosphor for White Light Emitting Diodes," *J. Eelctrochem. Soc.*, **152**, H168–171 (2005).

[10]R. T. Wegh, H. Donker, K. D. Oskam, and A., Meijerink, "Visible Quantum Cutting in $LiGdF_4$: Eu^{3+} Thorough Downconversion," *Science*, **283**, 663–6 (1999).

[11]M. Yu, J. Lin, Z. Wang, J. Fu, S. Wang, H. J. Zhang, and Y. C. Han, "Fabrication, Patterning, and Optical Properties of Nanocrystalline YVO_4: A (A = Eu^{3+}, Dy^{3+}, Sm^{3+}, Er^{3+}) Phosphor Films via Sol–Gel Soft Lithograph," *Chem. Mater.*, **14**, 2224–31 (2002).

[12]R. A. S. Ferreira, L. D. Carlos, R. R. Goncalves, S. J. L. Ribeiro, and V. D. Z. Bermudez, "Energy-Transfer Mechanisms and Emission Quantum Yields in Eu^{3+}-Based Siloxane-Poly(Oxyethylene) Nanohybrids," *Chem. Mater.*, **13**, 2991–8 (2001).

[13]Z. G. Lu, J. W. Wang, Y. G. Tang, and Y. D. Li, "Synthesis and Photoluminescence of Eu^{3+}-Doped $Y_2Sn_2O_7$ Nanocrystals," *J. Solid State. Chem.*, **177**, 3075–9 (2004).

[14]M. P. O. Wolbers, F. C. J. M. Veggel, B. H. M. S. Ruël, J. W. Hofstraat, F. A. J. Geurts, and D. N. Reinhoudt, "Novel Preorganized Hemispherands to Encapsulate Rare Earth Ions: Shielding and Ligand Deuteration for Prolonged Lifetimes of Excited Eu^{3+} Ions," *J. Am. Chem. Soc.*, **119**, 138–44 (1997).

[15]O. Lehmann, K. Kömpe, and M. Haase, "Synthesis of Eu^{3+}-Doped Core and Core/Shell Nanoparticles and Direct Spectroscopic Identification of Dopant Sites at the Surface and in the Interior of the Particles," *J. Am. Chem. Soc.*, **126**, 14935–42 (2004).

[16]J. X. Wan, Z. H. Wang, X. Y. Chen, L. Mu, and Y. T. Qian, "Shape-Induced Enhanced Luminescent Properties of Red Phosphors: $Sr_2MgSi_2O_7:Eu^{3+}$ Nanotubes," *Eur. J. Inorg. Chem.*, **20**, 4031–4 (2005).

[17]Z. G. Wei, L. D. Sun, X. C. Jiang, C. S. Liao, C. H. Yan, Y. Tao, J. Zhang, T. D. Hu, and Y. N. Xie, "Correlation Between Size-Dependent Luminescent Properties and Local Structure Around Eu^{3+} Ions in YBO_3:Eu Nanocrystals: an XAFS Study," *Chem. Mater.*, **15**, 3011–7 (2003).

[18]R. Chakrabarti, M. Das, B. Karmakar, K. Annapurna, and S. Buddhudu, "Emission Analysis of Eu^3: Cao–La_2O_3–B_2O_3 Glass," *J. Non-Cryst. Solids*, **353**, 1422–6 (2007).

[19]G. Tang, J. Q. Zhu, Y. M. Zhu, and C. Y. Bai, "The Study on Properties of Eu^{3+}-Doped Fluorogallate Glasses," *J. Alloys Compd.*, **453**, 487–92 (2008).

[20]C. J. Jia, L. D. Sun, F. Luo, X. C. Jiang, L. H. Wei, and C. H. Yan, "Structural Transformation Induced Improved Luminescent Properties for $LaVO_4$: Eu Nanocrystals," *Appl. Phys. Lett.*, **84**, 5305–7 (2004).

[21]S. S. Yao, Y. Y. Li, L. H. Xue, and Y. W. Yan, "Synthesis and Luminescent Properties of a Novel red-Emitting Phosphor $Ba_2ZnSi_2O_7:Eu^{3+}$, B^{3+} for Ultraviolet Light-Emitting Diodes," *Int. J. Appl. Ceram. Technol.* DOI: 10.1111/j.1744-7402.2009.02447.x. (2009).

[22]A. P. C. Satnta and S. F. Teles "Spectra Lux Software v.2.0 Beta, Photo." Quânticao Nanodispositivos, Renami, 2003.

[23]M. Kimata, "Four-Coordinated Co^{2+} Cation in $Ca_2CoSi_2O_7$," *Z. Kristallogr.*, **69**, 40–1 (1982).

[24]Y. Ochi, "Crystal Structure of Sr–Akermanite Glass–Ceramics," *Mater. Res. Bull.*, **41**, 1825–34 (2006).

[25]Y. Hao and Y. H. Wang, "Synthesis and Photoluminescence of New Phosphors $M_2(Mg, Zn)Si_2O_7$: Mn^{2+} (M = Ca, Sr, Ba)," *Mater. Res. Bull.*, **42**, 2219–23 (2007).

[26]J. W. Kaiser and W. Jeistchko, "Crystal Structure of the New Barium Zinc Silicates $Ba_2ZnSi_2O_7$," *Z. Krist-New Cryst. Struct.*, **217**, 25–6 (2002).

[27]Y. A. Malinovskii, "The Crystal Structure of $Ba_2CuSi_2O_7$," *Dokl.Akad. Nauk. SSSR*, **278**, 616–9 (1984).

[28]T. Joseph and M. T. Sebastian, "Microwave Dielectric Properties of $(Sr_{1-x}A_x)_2(Zn_{1-x}B_x)Si_2O_7$ Ceramics (A = Ca, Ba and B = Co, Mg. Mn. Ni)," *J. Am. Ceram. Soc.*, **93**, 147–54 (2010).

[29]A. M. Pires and M. R. Davolos, "Luminescence of Europium (III) and Manganese (II) in Barium and Zinc Orthosilicate," *Chem. Mater.*, **13**, 21–7 (2001).
[30]M. Y. Peng, Z. W. Pei, G. Y. Hong, and Q. Su, "The reduction of Eu^{3+} to Eu^{2+} in $BaMgSiO_4$ Eu Prepared in Air and the Luminescence of $BaMgSiO_4$:Eu^{2+} Phosphors," *J. Mater. Chem.*, **13**, 1202–5 (2003).
[31]F. Liebau, *Structural Chemistry of Silicates, Structure, Bonding and Classification*. Springer-Verlag, Berlin, 1985.
[32]R. D. Shannon, "Revised Effective Ionic Radii and Systematic Studies of Interactomic Distance Halides and Chalcogenides," *Acta Cryst. A.*, **32**, 751–67 (1976).
[33]Z. W. Pei, Q. Su, and J. Y. Zhang, "The Valence Change from Re^{3+} to Re^{2+} (Re = Eu, Sm, Yb) in SrB_4O_7:Re Prepared in Air and the Spectral Properties of Re^2," *J. Alloys Compd.*, **198**, 51–3 (1998).
[34]Y. C. Kang, Y. S. Chung, and S. B. Park, "Preparation of YAG: Europium Red Phosphors by Spray Pyrolysis Using a Filter-Expansion Aerosol Generator," *J. Am. Ceram. Soc.*, **82**, 2056–60 (1999).
[35]W. T. Carnall, P. R. Fields, and K. Rajnak, "Electronic Energy Levels in the Trivalent Lanthanide Aquo Ions. IV. Eu^3," *J. Chem. Phys.*, **49**, 4450–5 (1968).
[36]A. Tarafder, A. R. Molla, and B. Karmakar, "Processing and Properties of Eu^{3+}-Doped Transparent YAG ($Y_3Al_5O_{12}$) Nanoglass-Ceramics," *J. Am. Ceram. Soc.*, **93**, 3244–51 (2010).
[37]S. S. Yao, Y. Y. Li, L. H. Xue, and Y. W. Yan, "Luminescent Properties of $Ba_2ZnSi_2O_7$: Eu^{3+} Phosphors Prepared by Sol–Gel Process," *Eur. Phys. J. Appl. Phys.*, **48**, 20602, 4pp (2009).
[38]B. R. Judd, "Optical Absorption Intensities of Rare-Earth Ions," *Phys. Rev. B: Condens. Matter.*, **127**, 750–61 (1962).
[39]G. Blasse and B. C. Grabmaier, *Luminescent Materials*. Springer-Verlag, Berlin, Germay, 1994.
[40]S. Fujihara and K. Tokumo, "Multiband Orange-Red Luminescence of Eu^{3+} Ions Based on the Pyrochlore-Structured Host Crystal," *Chem. Mater.*, **17**, 5587–93 (2005).
[41]L. X. Yu, H. W. Song, S. Z. Lu, Z. X. Liu, L. M. Yang, and X. G. Kong, "Luminescent Properties of $LaPO_4$:Eu Nanoparticles and Nanowires," *J. Phys. Chem. B.*, **108**, 16697–702 (2004).
[42]Y. Nageno, H. Takebe, K. Morinaga, and T. Lzumitani, "Effect of Modifier Ions on Fluorescence and Absorption of Eu^{3+} in Alkali and Alkaline Earth Silicate Glasses," *J. Non-Cryst. Solids.*, **169**, 288–94 (1994).
[43]J. Lin and Q. Su, "A Study of Site Occupation of Eu^{3+} in $Me_2Y_8(SiO_4)_6O_2$ (Me = Mg, Ca, Sr)," *Mater. Chem. Phys.*, **38**, 98–101 (1994).
[44]G. Blasse, A. Bril, and W. C. Nieuwpoort, "On the Eu^{3+} Fluorescence in Mixed Metal Oxides: Part I—The Crystal Structure Sensitivity of the Intensity Ration of Electric and Magnetic Dipole Emission," *J. Phys. Chem. Sol.*, **27**, 1587–92 (1966).
[45]Z. G. Lu, L. M. Chen, Y. G. Tang, and Y. D. Li, "Preparation and Luminescence Properties of Eu^{3+}-Doped $MSnO_3$ (M = Ca, Sr, and Ba) Perovskite Materials," *J. Alloys Compd.*, **387**, L1–4 (2005). □